Synthesis of Pt-based alloy nanostructures

G.M. Leteba[1] and E. van Steen[1]

Affiliation:
[1] Catalysis Institute, Department of Chemical Engineering, University of Cape Town, South Africa.

Correspondence to:
E. van Steen

Email:
eric.vansteen@uct.ac.za

Dates:
Received: 30 Aug. 2020
Revised: 24 Mar. 2021
Accepted: 24 Mar. 2021
Published: June 2021

How to cite:
Leteba, G.M. and van Steen, E. 2021
Synthesis of Pt-based alloy nanostructures.
Journal of the Southern African Institute of Mining and Metallurgy, vol. 121, no. 6, pp. 283–286.

DOI ID:
http://dx.doi.org/10.17159/2411-9717/1345/2021

ORCID
G.M. Leteba
http://orcid.org/0000-0001-7982-5037

E. van Steen
http://orcid.org/0000-0003-4659-8522

Synopsis

Optimizing the catalytic performance of multimetallic nanoparticle (NP) catalysts demands a concrete understanding of their design, while preferentially deploying wet chemical synthesis procedures to precisely control surface structural properties. Here we report the influence of reductants such as hydrogen-rich tetrabutylammonium borohydride (TBAB) and carbon monoxide-rich molybdenum carbonyl ($Mo(CO)_6$) on the shape and morphological evolution of Pt-based binary (PtNi and PtCo) and ternary (PtNiAu and PtCoAu) nanostructures derived from a homogeneous solution of amine-based surface active agents (surfactants) in a high boiling point solvent. We successfully synthesized nanostructures exhibiting well-defined and composition-controlled surfaces deploying a one-pot synthetic approach. The development of the surface properties was, however, observed to be alloy-specific. The resultant highly monodisperse alloy NP with narrow size distributions and facet-oriented surfaces are expected to display enhanced functionality as catalysts for utilization in specific chemical reactions.

Keywords
catalyst. platinum alloy, nanoparticles, synthesis, mixed-metal nanostructure.

Introduction

Alloy nanoparticles (NPs), with core-shell or alloyed structures, are emerging as better catalyst candidates than monometallic NPs (Wang *et al*, 2019; Leteba *et al*., 2018). Bimetallic nanocatalysts are anticipated to exhibit unique properties as a result of their solid solution state (Wang *et al.*, 2019), and also to have unusual surface structures due to synergistic effects (Wang *et al*., 2019; Adams *et al*., 2009). A fundamental understanding of the structure-composition-activity relationships, *i.e.* how atomic arrangement influences performance, is a key to rational catalyst design for a particular reaction process at the nanoscale (Meunier, 2008). Detailed structural characterization of mixed-metal nanostructures for the investigation of the basic structural properties comprising size, shape, dispersion, purity, composition, and structure, is thus indispensable for their utilization in many industrial processes. The reliable synthesis of Pt-based nanostructures for high-performance applications is in great demand, but is more difficult to achieve than the synthesis of monometallic NPs (Wang and Li, 2011).

When two or more metal precursors are reduced simultaneously in a wet chemical synthetic route, they can thermodynamically nucleate and grow individually. This may result in the formation of either separate NPs, or hetero-structured or core-shell structures because of the differences in the standard reduction potentials. However, alloy NPs are formed in most cases (Shan *et al*., 2014). Simultaneous reduction of two or more metal precursor salts at nearly similar rates is achievable by using reductants at high temperatures in the presence of appropriate surface-active agents (surfactants) and solvents (Dumestre, 2004; Huang *et al*., 2009). Although the prime objective of introducing the surfactants into the synthetic system prior to the co-reduction of different metal precursors is to control growth of the particles, prohibit the formation of NP agglomerates, and limit the degree of NP oxidation, a homogeneous mixture of two or more surfactants can be also be used to promote anisotropic growth; hence the evolution of crystallographic-facet-directed solid solutions (Leteba *et al*., 2018, 2020). The evolution of high-index surfaces of these nanostructures can, however, be specific for a particular alloy system. Shape- and size-controlled growth of Pt-based alloy NPs can also be influenced by varying the reductants while keeping the other reaction conditions constant, but these reductants can influence the

evolution of different morphologies, sizes, and compositions, depending on their chemical nature and strength on inducing the reduction of metal precursors (Yin and Alivisatos, 2005; Chen *et al.*, 2018; Dahl, Maddux, and Hutchison, 2007; Wang *et al.*, 2007).

Here, we show that crystallographic-facet-directed alloy nanostructures can be formed via optimal solution-based synthetic methods by varying two distinct reductants in the presence of a homogeneous mixture of ternary surfactants – oleylamine (OAm), octadecylamine (ODA), and trioctylamine (TOA) – in a high boiling point solvent, benzyl ether (BE). These Pt-based binary nanoalloys were successfully synthesized by the simultaneous reduction of Pt and *M* (*M* = Ni and Co) precursor salts using carbon monoxide (CO)-rich molybdenum carbonyl ($Mo(CO)_6$) and hydrogen-rich tetrabutylammonium borohydride (TBAB) as the reductants. Good manipulation over sizes, morphologies, compositions, dispersity, and surface structures of these alloy NPs was obtained through rigorous control of the synthesis parameters such as the reduction temperature, concentration and type of the surfactants, distinct metal precursors, reaction time, and (most importantly) the reductants. It should be noted that a kinetic and/or mechanistic analysis of the particle growth was beyond the scope of this study.

Experimental

Synthesis of binary alloy NPs

In a typical synthesis, precursor salts $Pt(acac)_2$ (40 mg) and $Ni(Ac)_2.4H_2O$ or $Co(Ac)_2.4H_2O$ (24 mg) were dissolved in oleyl amine (OAm, 15 ml), trioctylamine (TOA,10 ml), and octadecyl amine (ODA, 4.4 g) (surfactants) using benzyl ether (BE, 20 ml) as a high boiling-point solvent. The resulting metal salt-surfactant-solvent reaction mixture was heated at 150°C for 5–10 minutes under vigorous magnetic stirring in a round-bottom flask. Upon addition of $Mo(CO)_6$ (60 mg), the resultant pale-yellow homogeneous solution turned dark purple with evolving cloudy smoke, suggesting the evolution of gaseous CO. The bulk organic synthesis mixture then turned dark brown during the heat-up process to 240°C, with a heating rate of 10°C/min. Alternatively, the introduction of TBAB (60 mg) resulted in the rapid formation of the dark brown colloidal solution. In both cases, the resultant colloidal mixtures were held at 240°C for 60 minutes. Thereafter, the colloidal medium was removed from the heat source and quenched using cold water to ensure minimal structural transformations during the cooling process. Subsequently, the as-synthesized NPs were extracted from the synthesis media through flocculation by adding excess absolute ethanol. After settling (typically 2–3 days), the excess organic solvents were decanted and the particles were further cleaned by re-suspending in absolute ethanol. This colloidal precipitation-purification process was performed 3–4 times. The black product was finally re-suspended in chloroform, yielding a dark brown colloidal suspension for all alloy NPs.

Synthesis of ternary alloy NPs

Precursor salts $Pt(acac)_2$ (40 mg) or $H_2PtCl_6.xH_2O$ (52 mg), $Ni(Ac)_2.4H_2O$ or $Co(Ac)_2.4H_2O$ (24 mg) and $HAuCl_4$ (12 mg) were dissolved in a mixture of OAm (15 ml), TOA (10 ml), and ODA (4.4 g) (surfactants) using BE (20 ml). The synthesis conditions and precipitation-purification processes were the same as those described in the previous section.

Results and discussion

The nature of the precursor salts, reduction temperature, reducing agents, and surfactants can dictate the nucleation and growth kinetics of metal NPs, hence influencing the final surface structural properties (size and shape). Depending on the nature of individual surfactant's functional group, the degree of adsorption of two or more surfactants on growing crystal surfaces within the organic synthetic system can differ (Yin and Alivisatos, 2005; Chen *et al.*, 2018; Dahl, Maddux, and Hutchison, 2007; Wang *et al.*, 2007). Furthermore, good manipulation of the nucleation and subsequent growth of solution-grown NPs often demands the use of some specific reducing agents or metal precursors (Dumestre, 2004; Huang *et al.*, 2009). In order to circumvent the formation of spontaneous separate or heterostructured NPs and to obtain homogeneous nucleation and subsequent crystal growth of two or more dissimilar metal atoms, the reaction kinetics must be accurately regulated to obtain well-defined and mixed solid solution NPs, which may be either ordered or disordered. Figure 1 displays the possible structures that can be obtained by the synthesis of binary and ternary nanostructures under precisely tuned synthesis parameters.

Here, we explore the influence of systematically varying the Pt precursor and reducing agent (reductant) components, on the preparation of the solid solution NPs. The reduction kinetics of Pt and *M* (Ni and Co) precursor salts were systematically influenced by introducing the reductants such as $Mo(CO)_6$ or TBAB into the bulk organic synthesis mixture. We used amine-containing surfactant mixtures (OAm, TOA, and ODA), which contain similar functional groups, for fine-tuning of composition, size distribution, monodispersity, and crystal faceting of the solid solution NPs. A high boiling-point solvent, benzyl ether (BE, boiling point: 298°C), served as a liquid phase for nucleation, growth, and controlled mixing of distinct metal atoms; hence providing an avenue for uniform crystal growth. Nanostructures prepared using $Mo(CO)_6$ are displayed in Figures 2a and b whereas those synthesized using TBAB are shown in Figures 2c and 2d.

Our synthesis strategies produced binary NPs exhibiting good monodispersity, distinct morphologies, and narrow size distribution, as revealed by the bright-field transmission electron microscopy (BR-TEM) images shown in Figure 2. Even though these binary alloys were synthesised under the same reaction parameters but only varying the reductants, the sizes and morphologies are different in all cases. This suggests that the formation of these nanoalloy particles can be dictated by the reaction parameters (such as temperature, concentration

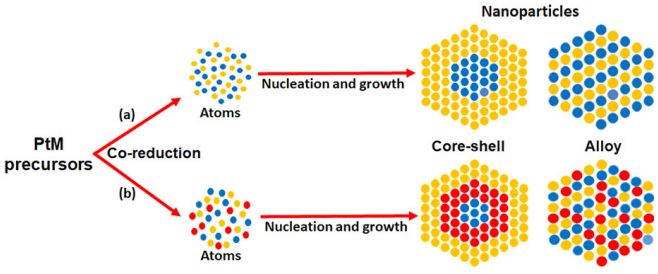

Figure 1—Illustration of possible nanostructures that can form during synthesis of (a) binary alloy nanostructures from two metal precursor salts and (b) ternary nanostructures from three metal precursor salts, under well-controlled reaction conditions

of both hydrophilic and hydrophobic surfactants, solvents, and metal precursors) and the nature of the reductants used during synthesis. The inserts in the figures are high-resolution-TEM (HR-TEM) images showing highly crystalline alloy nanostructures, and the same orientation of lattice fringes suggests that the individual particles are single crystals.

Figures 2a and 2b are BR-TEM- images of alloy nanostructures solution-grown by co-reduction of $Ni(Ac)_2.4H_2O$ (or $Co(Ac)_2.4H_2O$) and $Pt(acac)_2$ precursors using CO-rich $Mo(CO)_6$), which is the main source of CO gas. The resultant alloy particles display mostly cuboidal morphologies encased by {200} crystal facets. This is expected since previous studies have shown that the decomposition of $W(CO)_6$ results in the formation of W^0 while at the same time liberating gaseous CO. W^0 can then be used as a reductant, rapidly reducing Pt^{2+} to Pt^0 (atoms/seeds). This leads to fast Pt nucleation (Zhang and Fang, 2009; LaGrow *et al.*, 2015). However, W^0 does not alloy with Pt^0 under the reaction conditions and thus remains as an ionic species (W^{n+} or W^{6+}) in the organic synthesis mixture (Zhang and Fang, 2009), but facilitates growth of the nanoparticles (Zhang *et al.*, 2010). CO is known to adsorb selectively onto Pt, with stronger preferential binding on {100} facets and weaker adsorption on {111} facets (Wu, Zheng, and Fu, 2011; Chen *et al.*, 2012). Such preferential adsorption on Pt{100} crystal facets encourages the formation of cubic Pt and Pt alloy nanostructures (Wu, Zheng, and Fu, 2011; Chen *et al.*, 2012). Our studies indicate that $Mo(CO)_6$-assisted reduction of metal precursors is an applicable synthetic technique for the production of not only monodisperse NPs with a narrow size distribution, but also well-defined and facet-directed NP morphologies. It is therefore reasonable to conclude that $Mo(CO)_6$, similar to $W(CO)_6$, plays an essential role in the production of high-quality cuboidal alloy nanostructures. The NP uniformity obtained from the different metal salts to zero-valent metal states (Pt^0M^0) is expected to originate from the contribution of both CO gas and Mo0 species generated from the thermolytic decomposition of $Mo(CO)_6$, with Mo species serving as the sacrificial reductant in the nucleation stages of alloy NPs. The measured mean particle sizes from TEM images of randomly chosen 300 NP populations were 7.1 ± 0.5 nm (PtNi) and 12.5 ± 0.7 nm (PtCo), exhibiting narrow particle size distributions.

Simultaneous reduction of $Ni(Ac)_2.4H_2O$ (or $Co(Ac)_2.4H_2O$) and $Pt(acac)_2$ precursors using the H_2-rich reducing agent TBAB ($(C_{16}H_{36}N(BH_4))$) resulted in the production of predominantly spherical particles (Figures 2c and 2d). The measured average sizes of these binary NPs were 3.6 ± 0.9 nm (PtNi) and 4.5 ± 0.4 nm (PtCo), with narrow size distributions. Our studies indicate that TBAB-assisted reduction of metal precursors is a fast and facile synthetic approach for the formation of monodisperse small-sized NPs with a narrow size distribution. Based on these experiments, it is therefore reasonable to deduce that the co-reduction of metal precursors proceeds at a faster rate in the presence of reductant TBAB and nucleation of NPs thus occurs faster, followed by slow crystal growth. The significant influence of TBAB, resulting in synthesis of uniform small-sized NPs, could be associated with H_2 gas, which is released during the decomposition of TBAB and serves as a powerful reductant.

We also investigated the effect of the addition of a third metal component on size evolution and morphological selectivity of the alloy NPs. The simultaneous reduction of $Pt(acac)_2$ and $HAuCl_4$ in the presence of $Ni(Ac)_2.4H_2O$ and $Co(Ac)_2.4H_2O$, using $Mo(CO)_6$, produced ternary PtNiAu and PtCoAu alloy NPs displaying well-defined and uniform, near spherical morphologies, as shown in

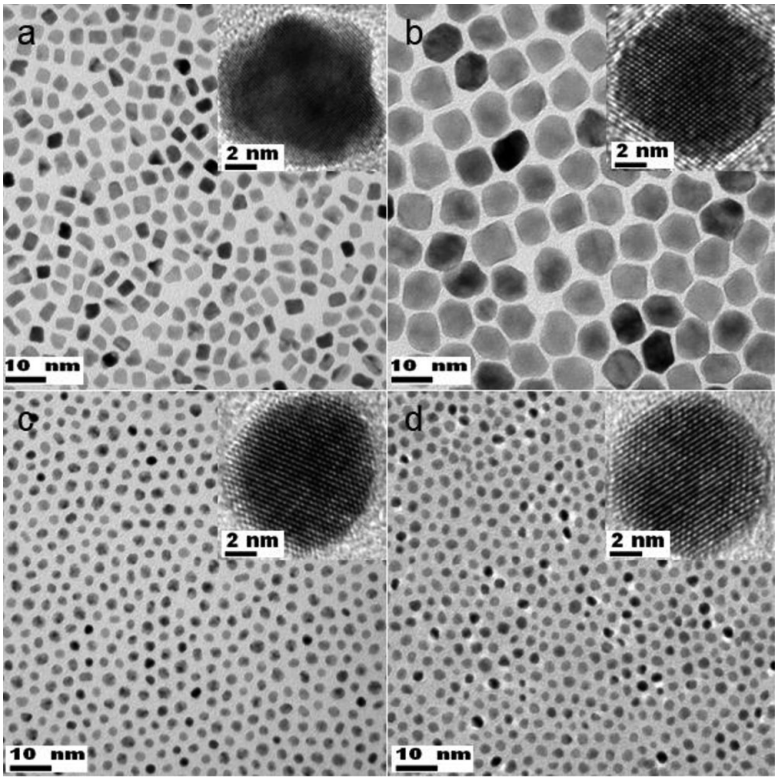

Figure 2—Bright-field TEM images of as-synthesised binary (a) PtNi and (b) PtCo bimetallic NPs using $Mo(CO)_6$ as a reducing agent. PtNi (c) and PtCo (d) were prepared using TBAB. The inserts show the HR-TEM images of these alloy NPs, displaying a high degree of crystallinity, and the same orientation of lattice fringes suggests that these particles are single crystals

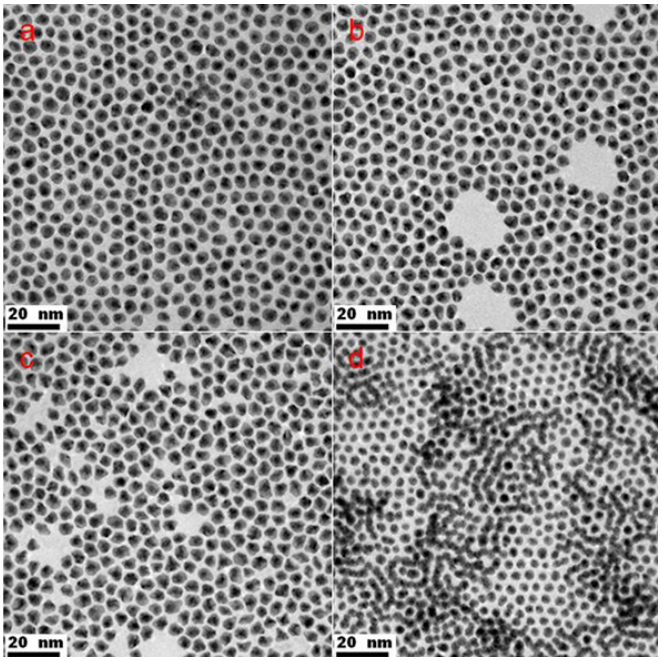

Figure 3—BF-TEM images of ternary (a) PtNiAu and (b) PtCoAu NPs obtained from the co-reduction of $Pt(acac)_2$ and $HAuCl_4$ in the presence of $Ni(Ac)_2.4H_2O$ and $Co(Ac)_2.4H_2O$ respectively, using $Mo(CO)_6$ as the reductant. (c) and (d) are TEM-BF images of PtNiAu and PtCoAu ternary NPs respectively, formed by substituting $Pt(acac)_2$ with $H_2PtCl_6.xH_2O$ under fixed experimental conditions and using $Mo(CO)_6$ reductant

Figures 3a and 3b, respectively. The measured mean edge lengths of these ternary NPs were PtNiAu 14.5 ± 0.9 nm and 14.7 ± 0.8 nm, displaying narrow size distributions. When $Pt(acac)_2$ was substituted with $H_2PtCl_6.xH_2O$ under fixed experimental conditions and using $Mo(CO)_6$ reductant, the PtNiAu system produced mostly irregular shapes, whereas the ternary PtCoAu system yielded spherical nanostructures as shown in Figures 3c and 3d, respectively. Thus, variation in Pt precursors did not result in any significant size and morphological differences between the ternary PtNiAu (average particle sizes 16.1 ± 1.2 nm) and PtCoAu (average particle sizes 10.7 ± 0.8 nm) systems. However, the cubic symmetry of binary alloy structures (Figures 3a and 3b) is broken, with the resultant ternary structures adopting spherical morphologies. This could be associated with the distinct chemical behaviour of Au, interfering with complete CO adsorption or contribution of Mo species on the nucleation stage of Pt.

Conclusion

Our findings clearly demonstrate the preparation of alloy nanostructures with distinct surfaces is achievable via precisely-controlled synthetic approaches. Good control over size, morphology, composition, dispersity, and surface structure of these alloy NPs was achieved using a one-pot synthetic approach and manipulating the experimental parameters. Although varying the reductants such as $Mo(CO)_6$ and TBAB under fixed reduction conditions resulted in the evolution of well-defined morphologies of binary (PtNi and PtCo) and ternary (PtNiAu and PtCoAu) NPs, these morphologies were found to be alloy-specific. This synthetic strategy to produce high-quality alloys of binary and ternary structures offers great potential for the successful synthesis of highly nanomaterials with controllable compositions to substitute pure Pt for use in current and future industrial applications.

Acknowledgement

This project was funded through the SARChI chair in Reaction Engineering (NRF grant number 114606).

Author contributions

Eric van Steen conceived the idea and supervised the project. Gerard Malefane Leteba synthesized nanoparticles. Gerard Malefane Leteba and Eric van Steen processed, interpreted TEM data and wrote the manuscript. All authors commented on the manuscript.

References

Adams, B.D., Wu, G., Nigro, S., and Chen, A. 2009. Facile synthesis of Pd–Cd nanostructures with high capacity for hydrogen storage. *Journal of the American Chemical Society*, vol. 131. pp. 6930–6931.

Chen, Y., Fan, Z., Zhang, Z., Niu, W., Li, C., Yang, N., Chen, B., and Zhang, H. 2018. Two-dimensional metal nanomaterials: Synthesis, properties, and applications. *Chemical Reviews*, vol. 118. pp. 6409–6455.

Dahl, J.A., Maddux, B.L.S., and Hutchison, J.E. 2007. Toward greener nanosynthesis. *Chemical Reviews*, vol. 107. pp. 2228–2269.

Dumestre, F. 2004. Superlattices of iron nanocubes synthesized from Fe[N(SiMe3)2]2. *Science*, vol. 303. pp. 821–823.

Huang, X., Zhang, H., Guo, C., Zhou, Z., and Zheng, N. 2009. Simplifying the creation of hollow metallic nanostructures: One-pot synthesis of hollow palladium/platinum single-crystalline nanocubes. *Angewandte Chemie International Edition*, vol. 48. pp. 4808–4812.

LaGrow, A.P., Knudsen, K.R., AlYami, N.M., Anjum, D.H., and Bakr, O.M. 2015. Effect of precursor ligands and oxidation state in the synthesis of bimetallic nano-alloys. *Chemistry of Materials*, vol. 27. pp. 4134–4141.

Leteba, G.M., Mitchell, D.R.G., Levecque, P.B.J., and Lang, C.I. 2018. Solution-grown dendritic Pt-based ternary nanostructures for enhanced oxygen reduction reaction functionality. *Nanomaterials*, vol. 8. p. 462. https://doi.org/10.3390/nano8070462

Leteba, G.M., Mitchell, D.R.G., Levecque, P.B.J., Macheli, L., van Steen, E., and Lang, C.I. 2020. High-index core–shell Ni–Pt nanoparticles as oxygen reduction electrocatalysts. *ACS Applied. Nano Materials*, vol. 3. pp. 5718–5731.

Meunier, F.C. 2008. Bridging the gap between surface science and industrial catalysis. *ACS Nano*, vol. 2. pp. 2441–2444.

Shan, S., Luo, J., Yang, L., and Zhong, C.J. 2014. Nanoalloy catalysts: Structural and catalytic properties. *Catalysis Science and Technology*, vol. 4. pp. 3570–3588.

Wang, C., Daimon, H., Lee, Y., Kim, J., and Sun, S. 2007. Synthesis of monodisperse Pt nanocubes and their enhanced catalysis for oxygen reduction. *Journal.of the American Chemical Society*, vol. 129. pp. 6974–6975.

Wang, D. and Li, Y. 2011. Effective octadecylamine system for nanocrystal synthesis. *Inorganic Chemistry*, vol. 50. pp. 5196–5202.

Wang, Y.-C., Slater, T.J.A., Leteba, G.M., Roseman, A.M., Race, C.P., Young, N.P., Kirkland, A.I., Lang, C.I., and Haigh, S.J. 2019. Imaging three-dimensional elemental inhomogeneity in Pt–Ni nanoparticles using spectroscopic single particle reconstruction. *Nano Letters*, vol. 19. pp. 732–738.

Wu, B., Zheng, N., and Fu, G. 2011. Small molecules control the formation of Pt nanocrystals: A key role of carbon monoxide in the synthesis of Pt nanocubes. *Chemical Communications*, vol. 47. pp. 1039–1041.

Yin, Y. and Alivisatos, A.P. 2005. Colloidal nanocrystal synthesis and the organic–inorganic interface. *Nature*, vol. 437. pp. 664–670.

Zhang, J. and Fang, J. 2009. A general strategy for preparation of Pt 3d-transition metal (Co, Fe, Ni) nanocubes. *Journal of the American Chemical Society*, vol. 131. pp. 18543–18547.

Zhang, J., Yang, H., Fang, J., and Zou, S. 2010. Synthesis and oxygen reduction activity of shape-controlled Pt3Ni nanopolyhedra. *Nano Letters*, vol. 10. pp. 638–644. ◆